

# **Does culture in the darkness effect retina morphology of *Sepia officinalis*?**

Rachael Warrington

Project Advisor: [John Spicer](#), School of Biological Sciences, University of Plymouth, Drake Circus, Plymouth, PL4 8AA

## **Abstract**

In *S. officinalis* there was no significant difference ( $P = 0.241$ ) for the eye diameter in terms of body length. The body length was significantly longer in cuttlefish reared in the dark treatment ( $P = 0.029$ ). This could be due to photoperiod regulating the release of growth hormones. The outer segment is similar in both treatments containing small compacted rhabdomeres elongating towards the inner segment. The dark retina has a thicker outer segment than the light, which could be an adaptation increasing the probability for photon capture by the rhabdomeres. Rhabdomeres vary little between treatments in comparison to vesicle cells and myeloid bodies. Rhabdomeres contract during illumination and elongate in the dark. The presence of myeloid bodies has been noted in the inner segment of the dark retina only. Myeloid bodies are said to transform into vesicle cells in the outer segment. A connection between pigment and vesicles has been suggested, however further research needs to be conducted on this area to determine their relation. Within the retina most of the variation occurred in the inner segment between treatments. The inner segment is thicker in the retina of the light sample which could be due to the need for photoproduct to synthesize rhodopsin under illumination. One of the biggest obstacles to overcome was achieving accurate orientation within the section of the sample. It is inconclusive whether the variation seen within the retina is due to the effect of darkness, due to the small sample size tested.

## Introduction

*Sepia officinalis* breed in shallow coastal waters during the spring and summer months (Naylor, 2005). Embryogenesis for *Sepia officinalis* lasts between 35 – 41 D in sea water  $T = 20^{\circ}\text{C}$  or 77 – 85 D at  $T = 15^{\circ}\text{C}$  (Fioroni, 1990). As with other cuttlefish, *S. officinalis* hatch as fully formed miniature adults (Groeger *et al.*, 2006). Their eyes are fully photosensitive before hatching (Yamamoto, 1985; Darmaillacq *et al.*, 2006; Darmaillacq *et al.*, 2008). At hatching the eyes are quite large (approximately 2.5mm in diameter or, 25% of the mantle length) (Groeger *et al.*, 2006) and the rhabdomeric layer is about a third the thickness of that found in the adult retina (Yamamoto, 1985). Having large eyes is an important feature as juveniles develop without parental care, enabling them to identify suitable prey and feed shortly after hatching, as their embryonic lipid reserves are short lived (Wells, 1958; Damailacq *et al.*, 2006). Cephalopods continue to grow throughout life. The eyes increase in size but at a slower rate than embryogenesis (adult eye diameter - 40 mm, 10% of mantle length in a mature male) (Groeger *et al.*, 2006). Visual acuity is better in large cuttlefish (Groeger *et al.*, 2005) due to possession of longer photoreceptors increasing the probability for photon capture (Land, 1981). Given the importance of vision in these animals, it is perhaps not surprising that much work has been done on eye development and the ontogeny of vision (Yamamoto, 1985; Fioroni, 1990; Meinertzhagen, 1990; West *et al.*, 1995; Boletzky *et al.*, 2006; Groeger *et al.*, 2006). Interestingly though a number of the morphological structures visible in such studies are not always described.

Rhodopsin is a visual pigment contained within rhabdomal membranes and is located in the outer segment of the retina (Hara & Hara, 1965). Retinochrome occurs in the inner segment; its photoproduct may be used to resynthesize rhodopsin (Hara *et al.*, 1967; Hara and Hara, 1972). During light adaption retinochrome is bleached to its photoproduct, hence less retinochrome occurs in the inner segment (Hara & Hara, 1976). The retinochrome may be transferred to another area within the retina. Light adapted animals have much more retinochrome in the outer segment than dark adapted individuals; the increase in concentration found in the outer segment may be associated with the decrease in the inner segment (Hara and Hara, 1976).

Previous work has been conducted on the affects of light regime on rhabdomes and pigments within the retina. Young (1962) focused on light and dark adaptation in the eyes of octopods, *Loligo* and *Sepia*, analysing the speed at which pigments migrate and the extent of rhabdome contraction during light adaptation. During dark adaptation pigment withdraws maximally and concentrates at the base of rhabdomes, with some remaining between rhabdomes. In light adaptation pigment emerges rapidly in the ventral region. Young concluded that rhabdomes shortened in length under illumination and elongated in the dark. Hara and Hara (1976) looked at distribution of photopigments within squid retina. In dark adapted retinas, retinochrome distributes equally between the inner and outer segments. During light adaptation retinochrome decreases in the inner segment and increases in the outer. They concluded that retinochrome moves from the inner segment to the outer segment during light adaptation. To my knowledge no work has been conducted on the effect of culturing *Sepia officinalis* in the darkness on retinal morphology. This is important to determine as it has been hypothesised that the arrangement of the retina is related to ecological characteristics (Young, 1962; Hara & Hara, 1976). By

assessing the effect on the retina, morphological adaptations to different habitats would be better understood.

Consequently the aim of the present study is to see if there is a morphological difference between the retinas of light and dark adapted embryonic cuttlefish. It is presumed that the dark adapted individuals will need to modify their visual system in order to find food upon hatching. However due to the limited exposure time, it is expected that there will be no morphological effect on the retina, as development of the eye starts at stage 19, by stage 27 they are fully developed and are photosensitive before hatching (Arnold *et al.*, 1974). As eggs were randomly collected the developmental stage of embryos was unknown, and could not be determined without compromising the viability of the eggs. Therefore the cuttlefish will not be subjected long enough for there to be a morphological effect from darkness.

## Materials And Method

*Sepia officinalis* eggs (n=150), attached to strands of seaweed, were collected by SCUBA divers from Babbacombe Bay (Depth = 15m, T = 16°C), Devon. Eggs were transported to the laboratory at the University of Plymouth in constantly aerated water from the collection site. On arrival eggs (and the piece of seaweed to which each was attached) were transferred haphazardly to a number of aquaria containing aerated, untreated sea water (S = 34 PSU, T = 15°C, 12:12 L:D regime).

Within 24 h of arrival, half of the aquaria were blacked-out using black plastic bags ('dark': experimental) and the other half remained untreated ('light': control). Due to lack of space samples were pseudo-replicated. Eggs were checked daily (under dim red light for the 'dark' treatment to prevent adaptation to light) for signs of disease and hatching. Sea water was changed bi-weekly. Due to difficulties in obtaining viable eggs only 10 hatchlings (5L, 5D) were used in the experiment described below. Immediately upon hatching appropriate morphometric measurements were made (eye diameter in horizontal plane, body length from caudal to rostral tip including the head, to the nearest mm). To compare eye diameter in terms of body length for treatments the following equation was used:

$$\frac{\text{Eye Diameter (mm)}}{\text{Body Length (mm)}}$$

A t-test was performed to look for differences between treatments, with the null hypothesis that the treatments are the same. Individuals were then euthanized with MS-222 (1000 mg/l for 15 minutes; blocking action potentials - ALPHARMA, 2001) decapitated and fixed in glutaraldehyde (2.5%) containing sodium cacodylate buffer (100mmol.l<sup>-1</sup> with 3% NaCl, pH 7.2). Once fixed, the left eye from each specimen was excised. Excess tissue which does not contain retina, such as the front of the eye and optic lobe, was removed and the lens extracted to allow satisfactory resin infiltration (Figure 1). The transversely halved eyes were twice rinsed (15min, then overnight) in buffer (sodium cacodylate, 100mmol.l<sup>-1</sup>, pH 7.2). Next day tissues were post fixed (OsO<sub>4</sub>, 2% cacodylate) for 2 h, and then rinsed twice (15 min each) with buffer. Fixed tissues were taken through a series of alcohol dehydrations: first 30%, 50%, 70% alcohol (in buffer) (15min each) and left in 90% ethanol overnight. Next day tissues were washed twice in 100% ethanol for 15 min. Dehydrated tissues

were placed for 24 h in a series of epoxy resins (agar low viscosity, 30:70, 50:50, 70:30, 100:0 x 3, resin/ethanol mix).

The resultant resin samples were embedded in a flat bed mould for examination using transmission electron microscopy (TEM). Each mould was placed in an oven ( $T = 60^{\circ}\text{C}$ ) overnight. Once polymerised, samples were cut in preparation for sectioning. A Reichert – Jung Ultracut microtome was used to section the samples. Samples were cut transversely with a glass knife (made with a Reichert knife maker) in order to display the rhabdomeres in the correct orientation. Glass knives were

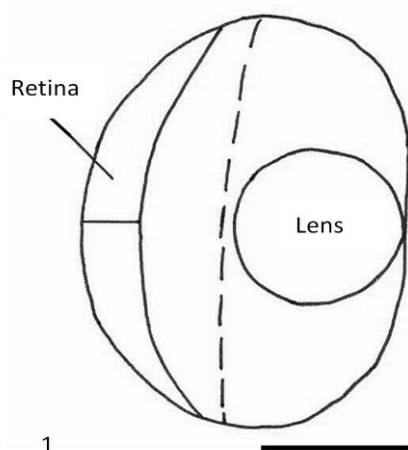


**Fig. 1** Cartoon of cuttlefish eye showing the lens and retina. The dotted line represents the dissection, discarding the front of the eye and lens, keeping the retina. The line located in the centre of the retina represents the transverse orientation which the retina should be cut. Scale bar = 500  $\mu\text{m}$ .

used for trimming and semi-thinning. To aid orientation slides were made of the retina and stained with Methylene Blue to view under low power (x4 and x10). Ultrathins (thickness = 90nm) were prepared for TEM using a diamond knife which is sharper than the glass knife. Producing gold coloured sections corresponding to the ultramicrotome section colour reference chart, this is the optimum section thickness which will provide good resolution to study the retina and good contrast for TEM observation (Khosravi-Far *et al.*, 2008). Sections were collected in a trough. Chloroform was waved slowly over the ultrathin sections to stretch them out as resin can suffer from compression (Dykstra & Reuss, 2003). Ultrathins were then mounted onto copper grids for use in TEM (Dykstra & Reuss, 2003).

Samples on copper grids were double stained, first with a saturated solution of uranyl acetate (70% ethanol), then with Reynolds lead citrate (Glauert, 1977). Copper grids were placed sample side down on a few droplets of uranyl acetate solution for 15 minutes, which were kept in the dark to prevent crystal formation as uranyl acetate is photosensitive (Khosravi-Far *et al.*, 2008). The copper grid was washed in distilled water and then dried on filter paper to remove the uranyl acetate stain as the solution is acidic, if any solution remains it will co-precipitate with the post stain – lead, producing crystals on TEM images (Dykstra & Reuss, 2003). Grids were then placed on drops of lead citrate for 15 min (the petri dish contained NaOH pellets to scavenge  $\text{CO}_2$  preventing lead precipitation, as lead is highly reactive with  $\text{CO}_2$ ) (Dykstra & Reuss, 2003). Grids were washed again in distilled water and dried

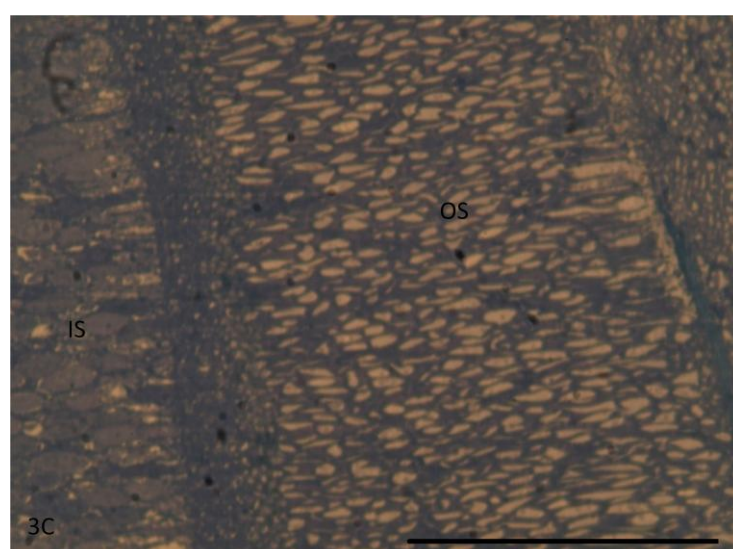
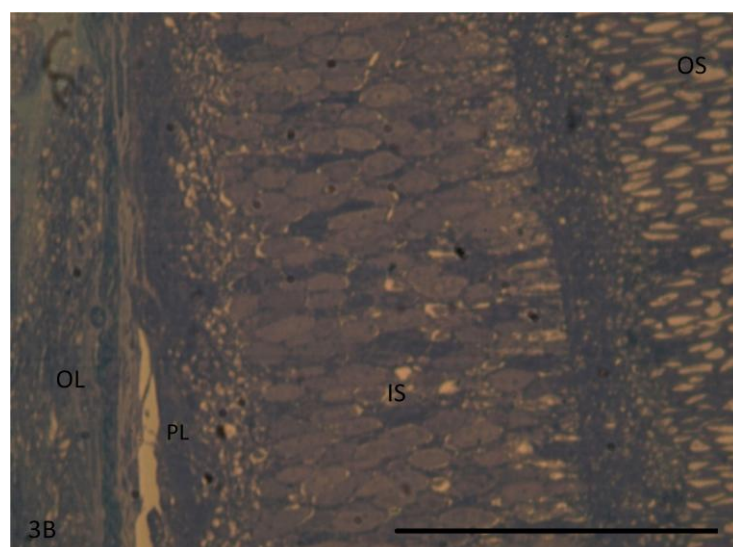
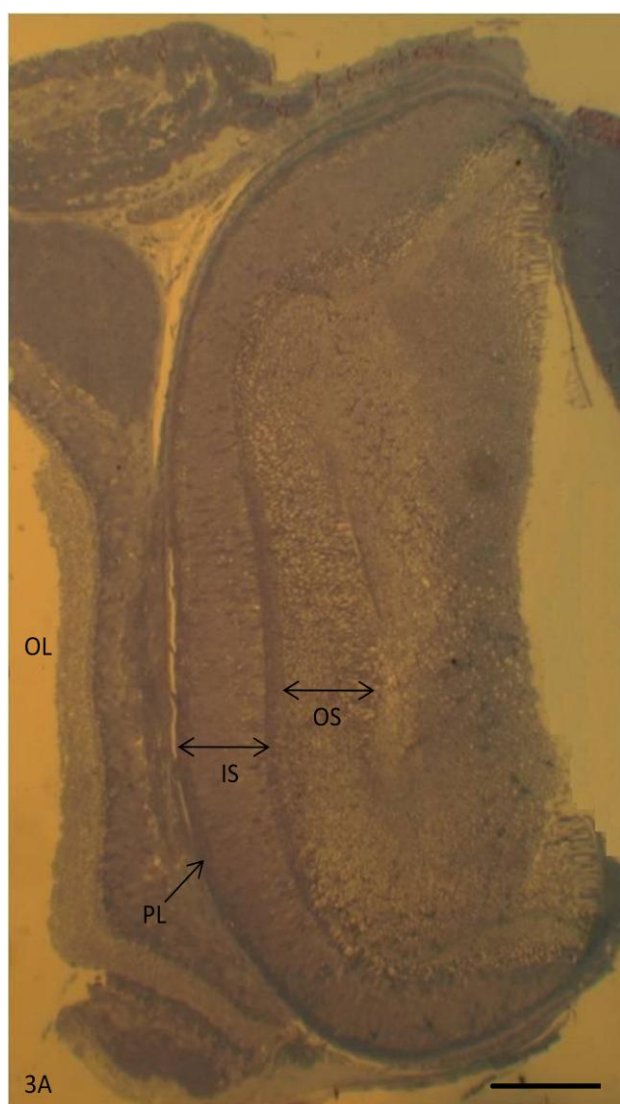


**Fig. 2** Light micrograph (Leica MZ6) of specimen reared in the light (A) excised cuttlefish eye (B) lens, mostly spherical apart from one side flattened. The dark tissue around the lens is where the lens was connected to the eye. (A) Scale bar = 100  $\mu$ m (B) Scale bar = 50  $\mu$ m.

**Fig. 3** Light micrographs of the retina of dark specimen. (A) Low powered picture of a section of whole cuttlefish eye. Scale bar = 200  $\mu$ m. (B) High powered micrograph inner segment of Figure 3A. Scale bar = 50  $\mu$ m. (C) High powered micrograph of outer segment of Figure 3A. Scale bar = 50  $\mu$ m. (IS) inner segment, (OL) optic lobe, (OS) outer segment, (PL) plexiform layer.

on filter paper. Lead citrate scatters electrons effectively, making the stain more intense (Dykstra & Reuss, 2003). These stains were used as the metal ions react chemically with some cellular components increasing their density which enhances the specimens contrast (Khosravi-Far *et al.*, 2008). Copper grids were placed in the JEOL – JEM 1200EX II TEM, to produce images of the samples. Light micrographs were taken with an Olympus E410 camera of the slides already prepared during sectioning to document the different layers, using a Leica DMIRB inverted light microscope.

## **Results**

### **Eye Diameter in terms of Body Length**

Cuttlefish hatched 52 – 63 days after collection. There was no significant difference in the eye diameter/body length ratio (range 9.1 – 16%) as a result of culture in the dark ( $t = 1.30$ ,  $DF = 6$ ,  $P = 0.241$ ). However there was a significant difference in body length between treatments ( $t = 2.75$ ,  $DF = 7$ ,  $P = 0.029$ ), those kept in the dark were longer ( $\bar{x} = 12.4\text{mm}$ ,  $ST = 0.89$ ) than those from the light ( $\bar{x} = 11\text{mm}$ ,  $ST = 0.71$ ). Consequently eye diameter on its own was compared between treatments, with no significant difference as a result of the experimental treatment ( $t = 0.45$ ,  $DF = 6$ ,  $P = 0.67$ ). In conclusion the difference in the eye/body length ratio was generated by a treatment effect on body length, not the eye per se.

### **Gross Morphology of Eye**

The eye does not appear to be spherical and shows some degree of dorso – ventral flattening (Figure 2A). The lens is spherical apart from flattening to one side (Figure 2B). A specimen from the dark treatment has been used to show the general structures which constitute the eye, as this was the best section produced from the study with the correct orientation (Figure 3A). Different layers within the retina can clearly be seen (Figures 3A, 3B & 3C). The main components of the retina are the outer and inner segments. The outer segment is comprised of rhabdomeres and supporting cell bodies (Figure 3C); while the inner segment comprises the receptor cell axons, nerve fibres, mitochondria, golgi, blood vessels and glial cells (Figure 3B).

### **Rhabdomeres**

As seen in this TS section light micrograph rhabdomeres are located in the outer segment of the retina (Figure 4). TEM shows microvilli of receptor cells which are orientated vertically and horizontally making up two opposite rhabdomeres (Figure 5).

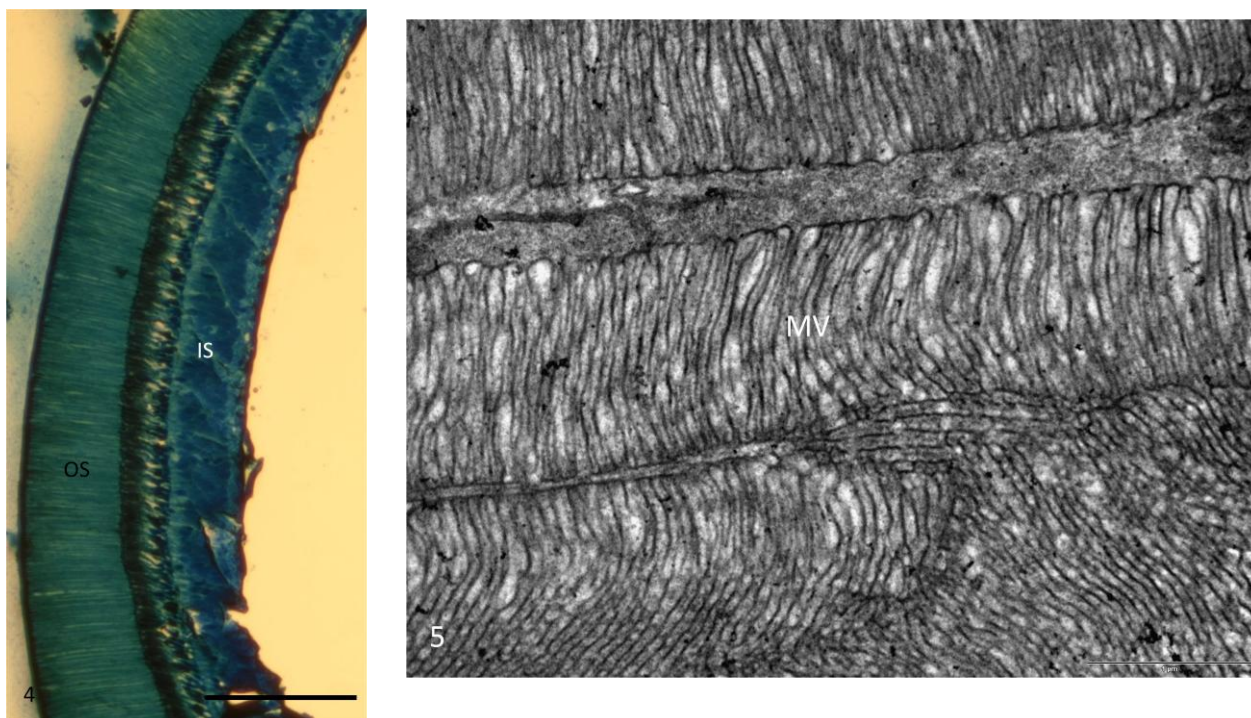


**Fig. 4** Light micrograph of dark sample to show the retina. The dark sample was used as this is the best orientation. (IS) inner segment (OS) outer segment. Scale bar = 100  $\mu$ m.

**Fig. 5** TEM image of dark sample (MV) microvilli of receptor cells forming rhabdomeres. Scale bar = 1  $\mu$ m.

### Light Treatment *versus* Dark

The light sample hatched 63 days after collection (ED = 1.5mm, BL = 11mm), while the dark sample hatched 56 days after collection (ED = 1.5mm, BL = 13mm). Light micrographs (Figure 6A & 6B) were used to compare differences, principally the retinal layers, in morphology as a result of rearing in the Light (L) or dark (D) conditions. Retina L has an outer segment which is 130  $\mu$ m and an inner segment of 120  $\mu$ m (Figure 6A). The outer segment of retina D by comparison measures 150  $\mu$ m while inner is 100  $\mu$ m (Figure 6B). Thus retina in individuals from the light treatment has a thicker inner segment by 20  $\mu$ m and a thinner outer segment by 20  $\mu$ m compared to those reared in the dark (Figure 6A & 6B). There is a pronounced difference between the widths of the outer and inner segments of the retina in the dark, as the inner segment is 2/3 the size of the outer segment (Figure 6B), compared to that of the light which has similar segment widths (Figure 6A). There is some evidence that orientation of the section tends to be better in retina D, as the differentiation between the segments is clearer than retina L (Figure 6A & 6B), which may slightly affect such comparisons. While light microscopy provided pictures of the different segments within the retina (Figure 7 & 13) the magnification was not good enough to visualise the structures within the layers. The location of each image taken with the TEM has been applied to the light micrographs (Figure 7 & 13), in order to see the arrangement that occurs within *Sepia officinalis* eye under each treatment.

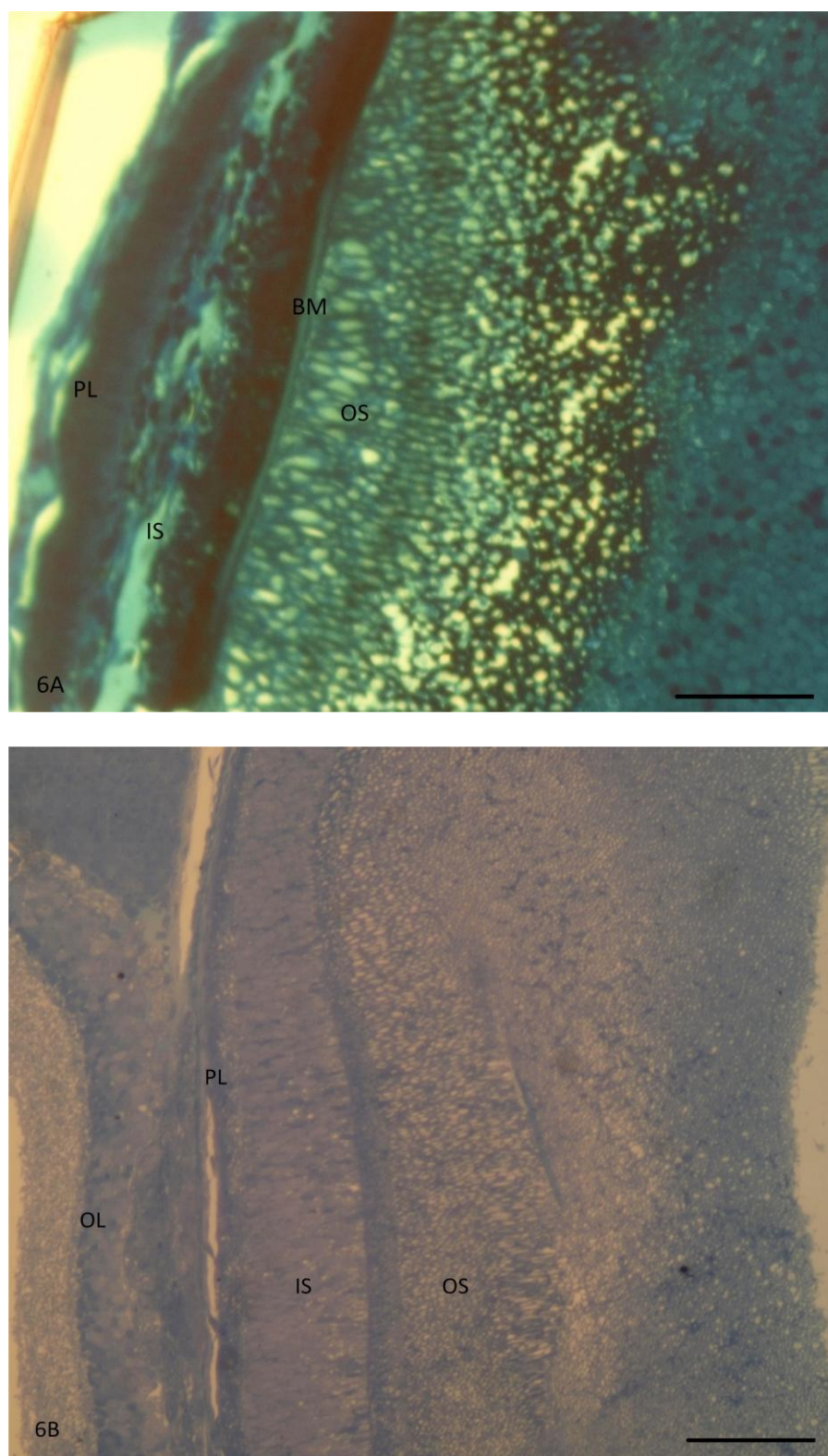


**Fig. 6** Light micrograph of the retina of a specimen reared in the light (A) and in the dark (B). (BM) basement membrane, (IS) inner segment, (OL) optic lobe, (OS) outer segment, (PL) plexiform layer, (SR) sub-rhabdomeric layer. Scale bar = 100  $\mu$ m.



## **TEM Analysis of the Light Treatment**

TEM transects describe layers found within the eye from the middle to periphery. The middle section contained an extensive amount of blood vessels, 8  $\mu\text{m}$  in diameter (Figure 8). Next occurred a nucleus layer 80  $\mu\text{m}$  thick (Figure 9). On the border of the outer segment a layer of vesicle cells 20  $\mu\text{m}$  wide was observed (Figures 10A, 10B & 11A). The outer segment is composed of rhabdomeres of varying shape and size (Figures 10A – 11C), being small and compact at the beginning of the outer layer (Figures 10A – 11A), elongating towards the basement membrane to 20  $\mu\text{m}$  in length (Figures 11A – 11C). The basement membrane layer divides the outer and inner segments, is acellular and 4  $\mu\text{m}$  thick. Highest concentrations of spherical and elongated vesicles occur at the start of the inner segment (Figure 11C, 11D & 11F); decreasing towards the plexiform layer. Also located within the inner segment are nucleuses (Figures 11C, 11E & 11F), glial cells (Figure 11D), and mitochondria (Figures 11E & 12). A membrane separates the inner segment from the plexiform layer, which is the periphery of the eye (Figure 11F).

## **TEM Analysis of the Dark Treatment**

A transect using TEM recorded layers in the dark treatment. Vesicle cells were found in the middle of the eye (Figure 14A). Encountered next was a dense collection of small rhabdomeres (Figure 14A & 14B), which continued for 100  $\mu\text{m}$ . These rhabdomeres were not included within the outer segment, as there seems to be a division between the dense collection of rhabdomeres and those found within the outer segment (Figure 13 see where (14C) is located). Rhabdomeres within the outer segment (150  $\mu\text{m}$  thick) elongate towards the inner segment to a length of 15  $\mu\text{m}$  (Figure 14C & 14D). A layer of vesicle cells occur after the rhabdomeres near the side of the eye (Figure 15). The sub-rhabdomic layer is 20  $\mu\text{m}$  wide; it contains receptor and supporting cells with vesicle cells occurring at the beginning of the layer (Figure 16A & 16B). Endoplasmic reticulum is found within receptor cells, while supporting cells contain nucleuses. The inner segment contains myeloid bodies (Figure 17A), microvilli, glial cells, receptor cells, supporting cells (Figure 18) and many blood vessels (Figure 17A & 17B) which elongate up to a length of 10  $\mu\text{m}$ . Longitudinally elongated nucleuses occur at the end of the inner segment (Figure 19), which is marked by a membrane (Figure 19). Within the plexiform layer mitochondria, longitudinal nucleuses and lamellated structures are observed (Figure 20). The plexiform layer is 8 $\mu\text{m}$  wide.

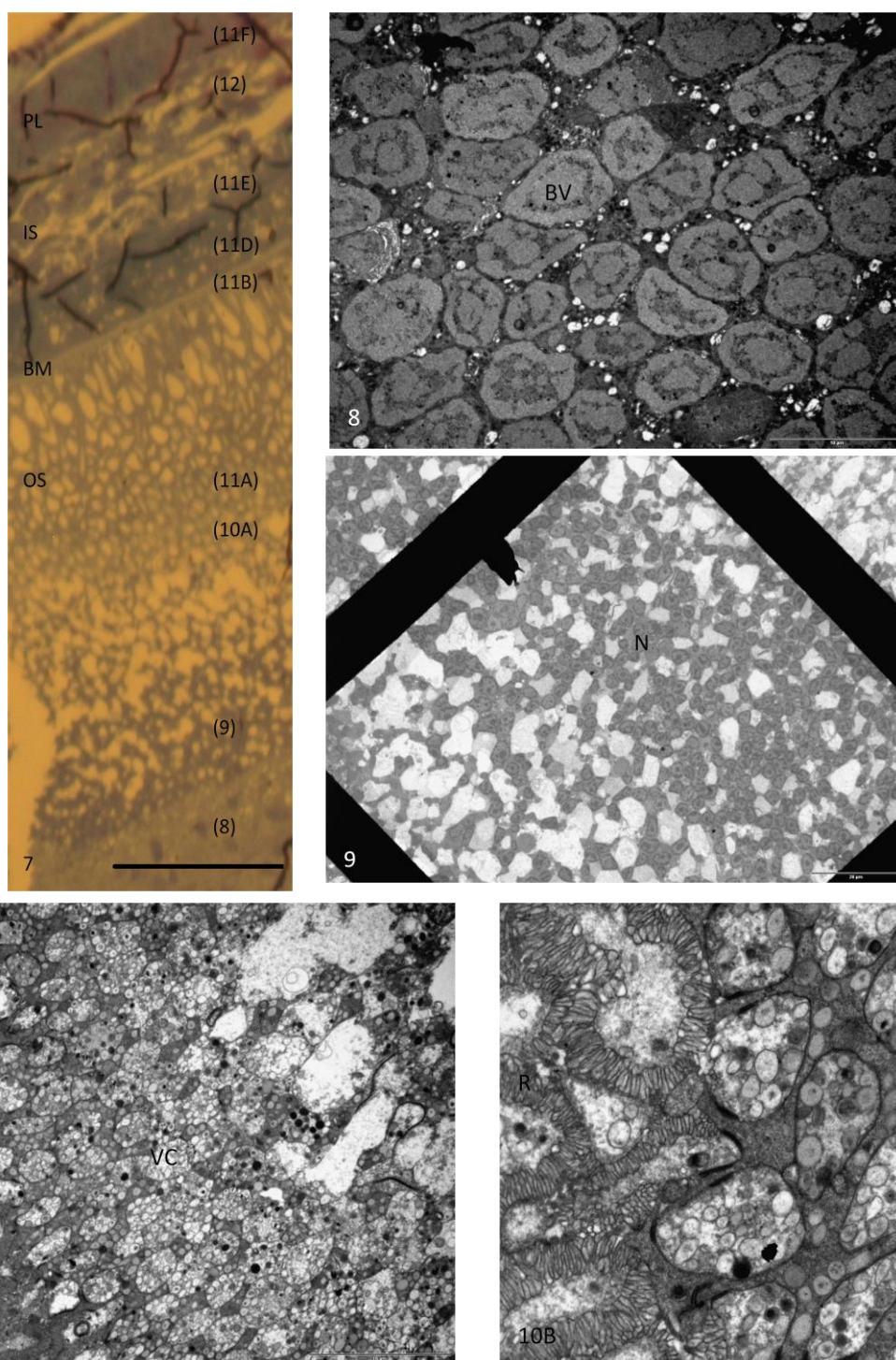


**Fig. 7** Light micrograph of the retina reared under the light treatment with focus on the segments and components found in the retina. numbers shown in brackets represent the figure which focuses in on the area. (IS) inner segment, (OS) outer segment, (PL) plexiform layer. Scale bar = 100  $\mu$ m.

**Fig. 8** TEM image of a layer of (BV) blood vessels in the outer segment. Scale bar = 10  $\mu$ m

**Fig. 9** TEM image of a layer which comprises many (N) nucleus, this is found next to the blood vessel layer. Scale bar = 20  $\mu$ m.

**Fig. 10** TEM images of the start of the outer segment. (A) The rhabdomeres are compacted at the beginning of the outer segment. Scale bar = 10  $\mu$ m. (B) Magnified view of the vesicle cells. Scale bar = 2  $\mu$ m. (R) rhabdomeres, (VC) vesicle cells.

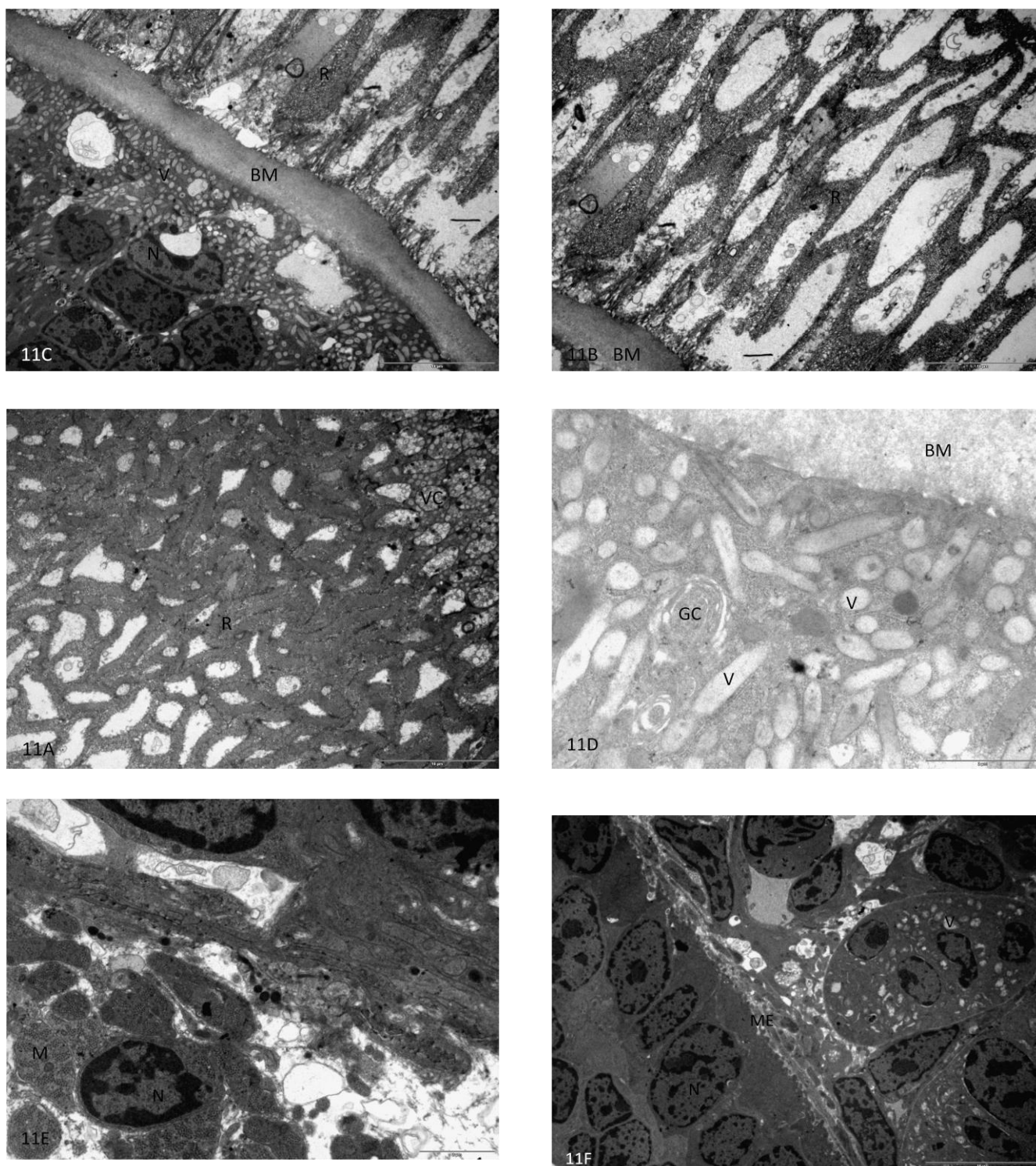


**Fig. 11** TEM images of the light reared specimen. (A) Outer segment. Scale bar = 10  $\mu\text{m}$ . (B) End of outer segment containing elongated rhabdomeres. Scale bar = 10  $\mu\text{m}$ . (C) Basement membrane displaying the inner and outer segments either side. Scale bar = 10  $\mu\text{m}$ . (D) Magnified view of the inner segment containing vesicles. Scale bar = 2  $\mu\text{m}$ . (E) Inner segment. Scale bar = 2  $\mu\text{m}$ . (F) Membrane separating the inner segment from the plexiform layer. Scale bar = 10  $\mu\text{m}$ . (BM) basement membrane, (GC) glial cells, (M) mitochondria, (ME) membrane, (N) nucleus, (R) rhabdomere, (V) vesicle, (VC) vesicle cell.

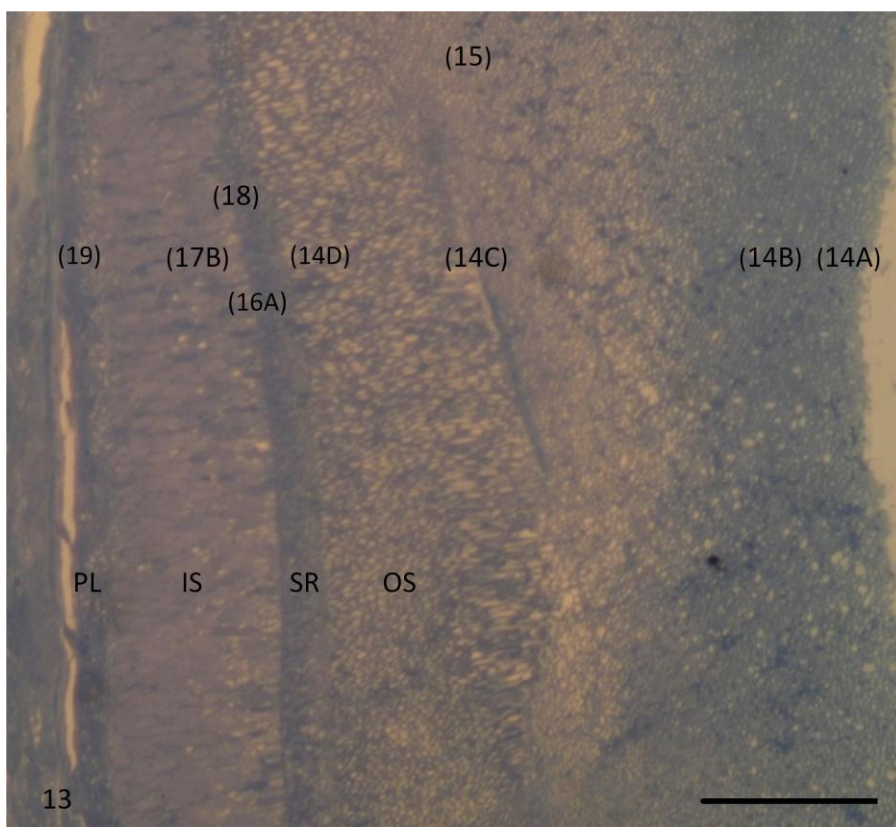
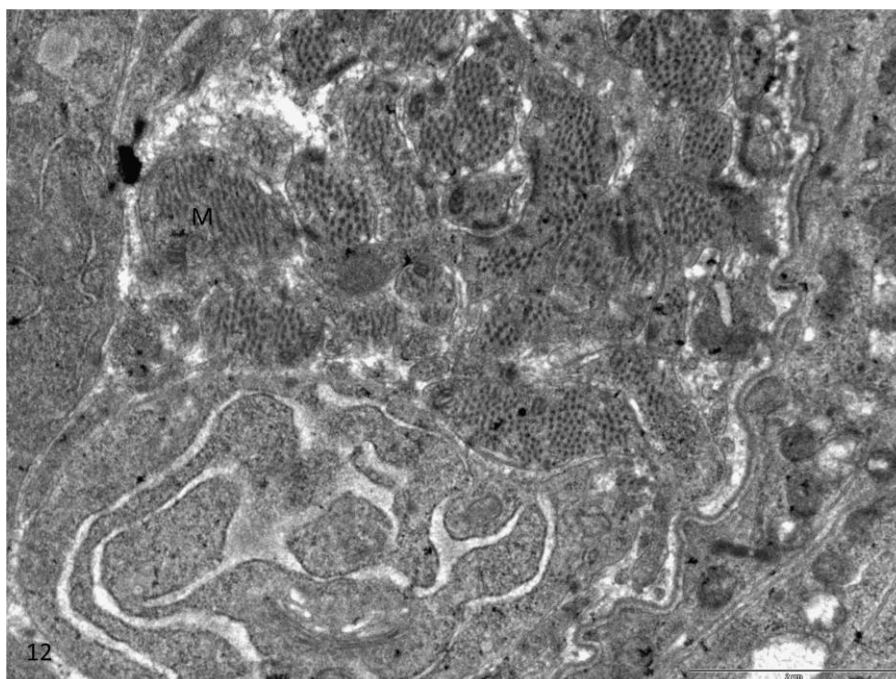


**Fig. 12** TEM image of the inner segment showing many (M) mitochondria. Scale bar = 2  $\mu$ m.

**Fig. 13** Light micrograph of the segments present within the eye of the specimen reared in the dark. The numbers in brackets correspond to the figures which displays a TEM image for the area of interest. The different areas shown are the (IS) inner segment, (OS) outer segment, (PL) plexiform layer, (SR) sub-rhabdomeric layer. Scale bar = 100  $\mu$ m.

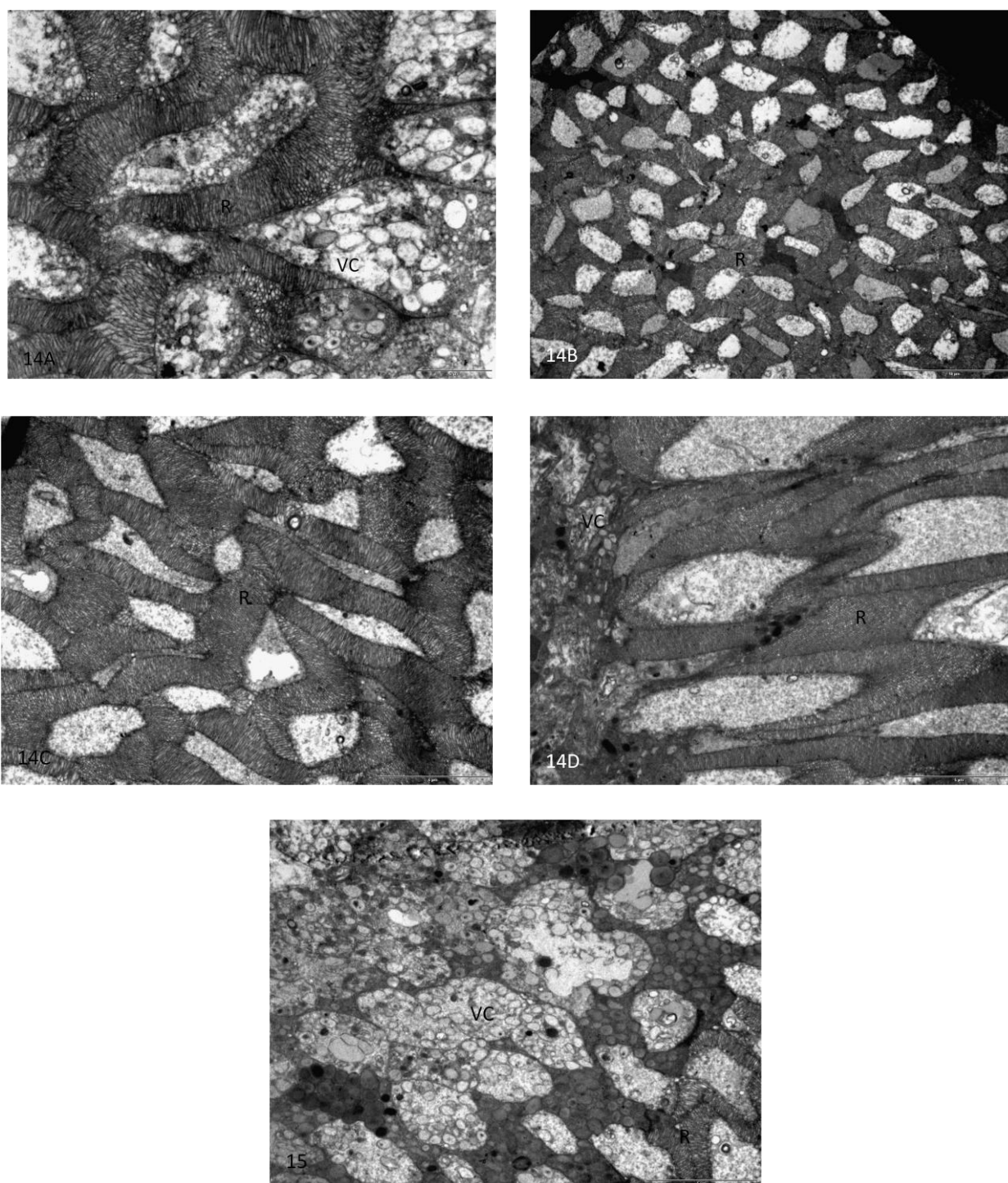


**Fig. 14** TEM image of the dark reared retina. A transect through the retina started in the middle of the eye working through the outer segment. (A) Start of outer segment. Scale bar = 2  $\mu\text{m}$ . (B) Small compacted rhabdomeres at beginning of outer segment. Scale bar = 10  $\mu\text{m}$ . (C) Middle of the outer segment as rhabdomeres start to elongate. Scale bar = 5  $\mu\text{m}$ . (D) End of outer segment and beginning of sub-rhabdomeric layer. Scale bar = 5  $\mu\text{m}$ . (R) rhabdomeres, (VC) vesicle cells.

**Fig. 15** TEM image of vesicle cells which on the edge of the outer segment, near the side of the eye. (R) rhabdomeres, (VC) vesicle cells. Scale bar = 5  $\mu\text{m}$ .

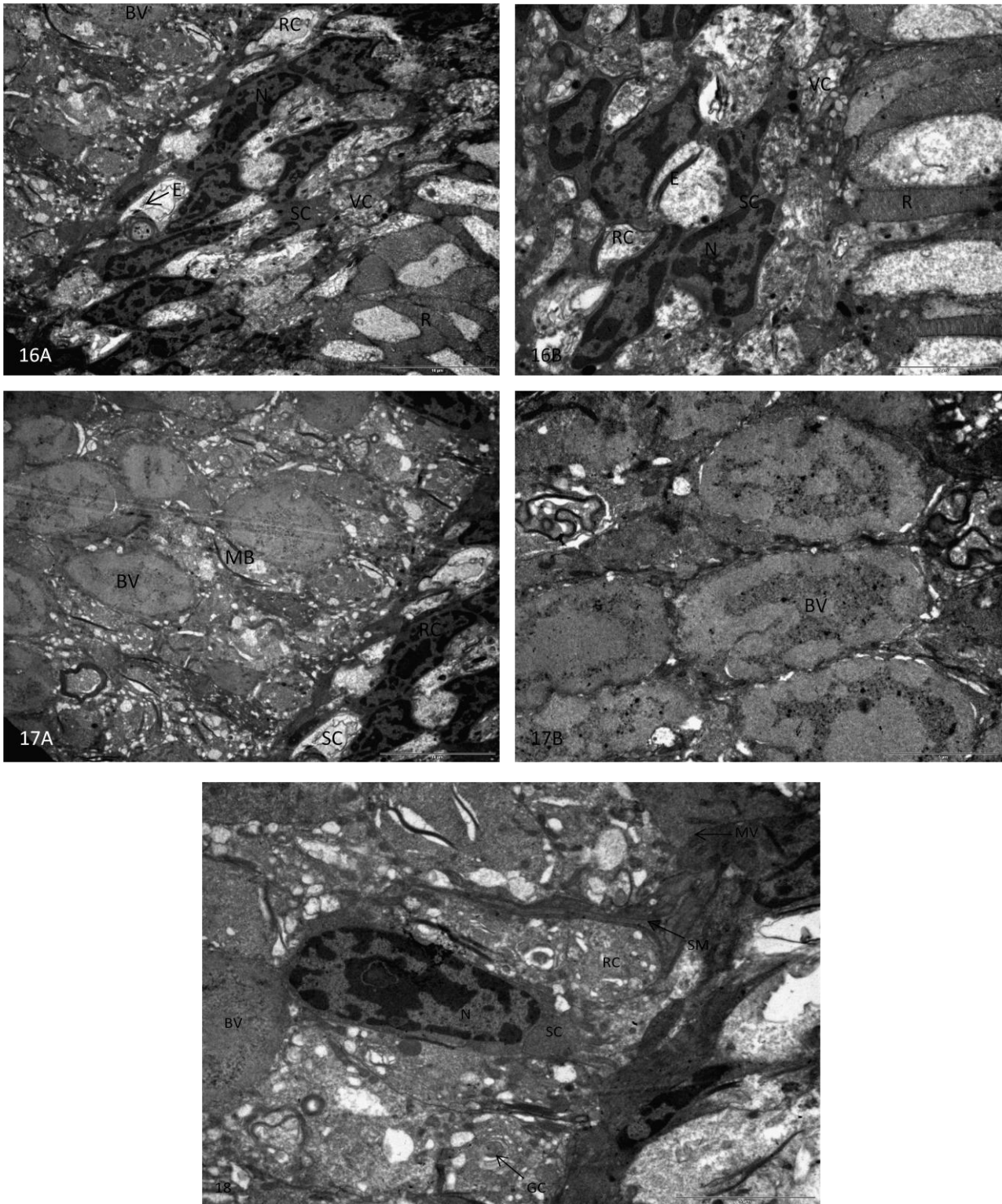


**Fig. 16** TEM images of the sub-rhabdomeric layer showing the segments surrounding. The outer segment contains the rhabdomeres while the inner segment contains blood vessels. (A) Scale bar = 10  $\mu\text{m}$ . (B) Scale bar = 5  $\mu\text{m}$ . (BV) blood vessel, (E) endoplasmic reticulum, (N) nucleus, (R) rhabdomeres, (RC) receptor cell, (SC) supporting cell, (VC) vesicle cell.

**Fig. 17** TEM image of the inner segment containing blood vessels. (A) Scale bar = 10  $\mu\text{m}$ . (B) Scale bar = 5  $\mu\text{m}$ . (BV) blood vessel, (MB) myeloid bodies, (RC) receptor cell, (SC) supporting cell. **Fig. 18** TEM image of the start of the inner segment with prime focus on a supporting cell and receptor cell. The supporting cell contains a nucleus. Microvilli of supporting cell can be seen next to a receptor cell. (BV) blood vessel, (GC) glial cell, (MB) myeloid bodies, (MV) microvilli projections, (N) nucleus, (R) rhabdomere, (SC) supporting cells, (SM) microvilli of supporting cell. Scale bar = 5  $\mu\text{m}$ .

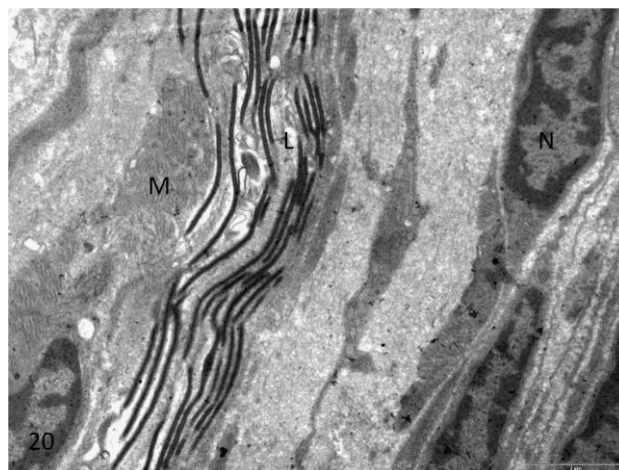
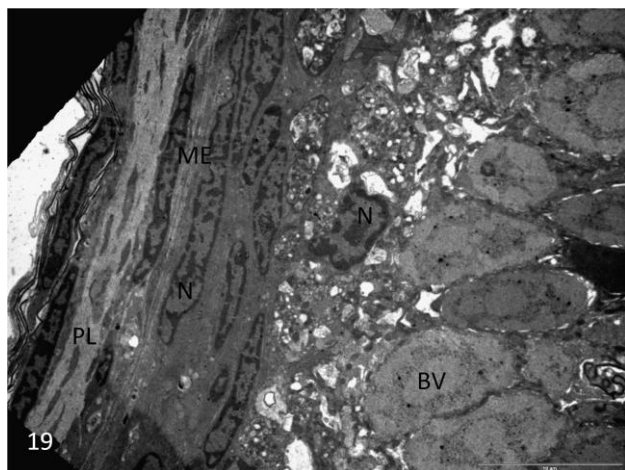


**Fig. 19** TEM image of the inner segment containing blood vessels and nucleuses. A membrane divides the inner segment and plexiform layer. (BV) blood vessel, (ME) membrane, (N) nucleus, (PL) plexiform layer. Scale bar = 10  $\mu\text{m}$ .

**Fig. 20** TEM image of the plexiform layer with few nucleuses. (L) lamellated structures, (M) mitochondria, (N) nucleus. Scale bar = 2  $\mu\text{m}$ .

## Discussion

### Eye Diameter in terms of Body Length

There was no difference in eye diameter/body length ratio between the treatments, demonstrating that the eyes are proportionally to the body length. Dark samples were shown to have longer bodies, which could be due to an increased feeding frequency on their lipid reserves, this has been documented to enhance growth even in a short photoperiod (Koueta & Boucaud-Camau, 2003). The photoperiod affects growth hormones, which could account for the observed difference (Björnsson, 1997). Body length is an unreliable measurement, varying on the mood of the animal (Steve O'Shea, personal communication). Better accuracy could be achieved by measuring the animal under a microscope (accurate to nearest  $\mu\text{m}$ ) after anaesthetising when muscles are relaxed.

### Rhabdomeres

The largest difference between treatments occurred in the middle of the eye; however this is not the prime concern of this study, suggesting that future work could be conducted within this area. TEM analysis portrays clear differences between the retinas of the treatments. With similarity occurring between the treatments in the outer segment; both possessing rhabdomeres which elongate towards the inner segment. In the illuminated sample the elongated rhabdomeres were longer by 5  $\mu\text{m}$ . Kalil (1978) documented that retinal morphology and physiology of cats are affected by rearing in darkness, initially retarding cell growth up to 25% compared to light reared cats. However after 16 weeks the size difference was reversed by a resumption of cell growth. Similar scenario might have occurred in the dark

treatment, resulting in initial retardation of rhabdome growth in *S. officinalis*, hence the light sample possesses longer rhabdomeres until adaptation to the dark rearing occurs, demonstrating that the dark sample could not adapt quick enough as the time for adaptation was limited to the embryonic period (once hatched they were killed). Differences in length or rhabdomes could be due to the treatments placed under.

Rhabdomeres occur in an orthogonal arrangement providing the basis of polarized light sensitivity (Hanlon & Messenger, 1998). Even though rhabdomeres are longer in the outer segment of the light sample, the dark possesses a thicker outer segment by 20  $\mu\text{m}$ . During photon limitation there will be selective pressure to maximise sensitivity to the available light (Turner *et al.*, 2009). Expanding the photoreceptive layer could be an adaptation to the complete darkness, increasing the chance to discriminate linear polarized light, helping the dark sample to perceive its environment. Young (1962) documented that the rhabdomes contract under illumination and elongate in the dark, which is in agreement with the present study, the function of these changes are unknown.

### **Variation between Segments**

Within the retina most variation occurs between the inner segments of the samples. The light treatment contains vesicles, nuclei, glial cells and mitochondria, whereas blood vessels and myeloid bodies are confined within the dark treatment. Literature states that the inner segment contains the nucleus, mitochondria and all the mechanisms necessary for cell maintenance (Pepe, 2001), with their abundance dependant on the state of adaptation (Hariyama *et al.*, 1986). The inner segment is larger in the light adapted retina by 20  $\mu\text{m}$ . This could be due to cuttlefish using up their visual pigment (rhodopsin) quicker in the light retina than the dark, making the inner segment thicker to enable the photoproduct of retinochrome to resynthesize rhodopsin efficiently. Differences observed between the inner and outer segments suggest that the variation could be due to adapting to the treatments light condition. Although this cannot be confirmed until further work has been conducted analysing more samples.

Differences between the widths of the segments in the dark treatment are pronounced, with the outer segment 50% larger than the inner segment, this could be a dark adaptation extending the outer segment to expose the rhabdomeres to more light. Similar sized segments occur in the light treatment, with only 8% difference, these segments do not need to be of differing sizes as light adaptation has already occurred.

### **Vesicles and Myeloid Bodies**

Previous micrographs (Yamamoto *et al.*, 1965) displaying pigment granules could not be confirmed in this study. This could be due to displacement from the light condition, or differences in the plane of section despite attempts to follow similar protocols. Other structures associated with the visual pigment have been noted in this study, such as vesicles and myeloid bodies.

Myeloid bodies are concerned with pigment regeneration (Muntz & Wentworth, 1987). Hara and Hara (1976) suggested that retinochrome synthesised in the inner segments are transferred across the basement membrane, to the basal region of the outer segment within myeloid bodies. Within the outer segment the retinochrome



interacts with metarhodopsin to promote the regeneration of rhodopsin. Myeloid bodies were only observed in the inner segment of the dark section. It is unlikely they are absent from the light section as they are needed for pigment regeneration, it could be that they are displaced elsewhere within the eye (Muntz & Wentworth, 1987). Hara and Hara did not find myeloid bodies present within the outer segment; they suggested myeloid bodies are transformed in the outer segment into smaller vesicles convenient for carrying retinochrome. The vesicles are presumed to be those which were found within the light and dark treatment of the present study, as literature does not illustrate their occurrence.

Vesicle cells were located by small compacted rhabdomeres of the outer segment in both treatments; with a thicker layer occurring in the light. Rhabdomeres contain a small amount of vesicles, which differs in direction for the treatments. The present study found that the light retina displayed vesicles at the base of elongated rhabdomes of the outer segment, while the opposite was found in dark retina with vesicles occurring in small compacted rhabdomes closest to the vesicle cells in the outer segment. If vesicles found within rhabdomes are associated with pigment this contradicts what Young (1962) concluded; during light adaptation pigment emerges from the ventral region and in dark adaptation pigments withdraw to the base of rhabdomes. Further work needs to be conducted into the association of vesicles to the pigment.

Previous studies demonstrate that during light adaptation the concentrations of retinochrome increase markedly in the outer segment (Hara & Hara, 1976; Young, 1962), which is in agreement with the present study, as more vesicles occur in the outer segment of the light retina. However it is odd that vesicles are present in the outer segment of the dark treatment, suggesting that the dark treatment could have been exposed to the light during fixation. Young (1962) documented that rhabdomes can change shape and pigments migrate after the eyes have been excised, which could explain the presence of vesicles in the outer segment of the dark specimen.

The dark section also contained vesicles within supporting cells of the sub rhabdomeric layer, with none occurring in the inner segment. Young (1962) acknowledged pigment to occur in supporting cells, which supports the theory that the vesicles contain pigment or are indeed the pigment. The light retinas inner segment contained spherical and ellipsoidal vesicles which are not found in the dark, the highest concentration occurred adjacent to the basement membrane. Yamamoto and colleagues (1965) noted the same occurrence but for pigment granules, providing more evidence that vesicles in the present study relate to pigment. If vesicles are related to pigment described in literature (Yamamoto *et al.*, 1965), it is odd that they do not occur in the inner segment as retinochrome is more abundant in dark retinas, due to reduced retinochrome within inner segments from bleaching, shifting retinochrome to outer segment during light adaptation (Young, 1962).

### **Theories on Variation**

Variations between light and dark samples could be explained in a number of ways. First, it could be due to environmental conditions, suggesting rearing in darkness does affect retinal morphology, relating arrangement of the retina to habitat (Young, 1962; Hara & Hara, 1976). Second, orientation could produce discrepancies when comparing samples, as comparatively simple structures can generate most or all of the different appearances depending on the plane of section (Muntz & Wentworth, 1987). Third, it could be due to chance, animals studied could be different due to

variability in pre-experimental conditions, differing between the collection sites. Fourth, the samples hatched at different times, the light sample hatched 7 days after the dark, lengthening the embryonic development of the light sample. Fifth, the differences seen could be due to specimens being placed under experimental conditions at different stages of development. As the animal gets closer to the time of hatching the morphological effect of darkness on the retina decreases, as embryos are fully photosensitive before hatching (Yamamoto, 1985; Darmaillacq *et al.*, 2006; Darmaillacq *et al.*, 2008).

## **Summary**

Limited literature is available on the effects of constant dark rearing on the visual system. The studies which have been made had mixed results and are mainly conducted on fish (Saszik & Bilotta, 2001). Literature biases towards the retina, rhabdomes, pigment and segments, while other structures remain unspecified, making identification difficult. Some features described in the literature are not visible on images from the present study, which could be due to orientation, e.g. the appearance of myeloid bodies varies widely from wavy membranous structures to complex loops, whorls and circles depending on the orientation (Muntz & Wentworth, 1987). The largest obstacle to overcome was obtaining the correct orientation. During sectioning protocols were followed to achieve transverse slices of the retina, despite all efforts the plane of section was not identical. To be directly comparable orientation needs to be improved. Accurate orientation could be achieved by mounting a fragment of retina (with the use of a small needle) onto cardboard before fixation, allowing transverse orientation to be determined prior to polymerisation of resin TEM use.

Further work needs to be conducted into the effect of darkness on the morphology of the retina as the present experiment had limited time and sample size. It is not conclusive whether the retina is affected by rearing in complete darkness, even though images provide evidence of differences, this cannot be fully accepted due to the problems of orientation and the small sample size. It would be interesting to analyse ontogenic effects from rearing in the darkness, as the eye of cuttlefish continues to grow after hatching, extending the time for adaptation to occur (Groeger *et al.*, 2006).

## **Acknowledgements**

I thank John I. Spicer and Roddy Williams for their valuable advice. Glenn Harper, Roy Moate and Peter Bond from the Electron Microscope Centre, for their technical help, guidance and advice while using the facilities. Ann Torr and Stefanie Broszeit for their help while using the laboratory. James Neighbour for collecting the cuttlefish eggs. Finally Gary Warrington for transportation of the eggs.

## References

**ALPHARMA.** (2001) MS 222 (Tricaine Methane Sulphonate) Technical Bulletin, pp. 6.

**Arnold J.M., Summers W.C., Gilbert D.L., Manalis R.S., Daw N.W. and Lasek R.J.** (1974) Embryonic development. In *A guide to laboratory use of squid Loligo pealei*. Woods Hole, MA: Marine Biological Laboratory, pp. 74.

**Björnsson B.T.** (1997) The biology of salmon growth hormone: from daylight to dominance. *Fish Physiology and Biochemistry* 17, 9-24.

**Boletzky S.V., Erlwein B. And Hofmann D.K.** (2006) The *Sepia* egg: a showcase of cephalopod embryology. *Life and Environment* 56. 191 – 201.

**Darmaillacq A.S., Chichery R., Shashar N. And Dickel L.** (2006) Early familiarization overrides innate prey preference in newly hatched *Sepia officinalis* cuttlefish. *Animal Behaviour* 71, 511 – 514.

**Darmaillacq A.S., Lesimple C. and Dickel L.** (2008) Embryonic vision learning in the cuttlefish, *Sepia officinalis*. *Animal Behaviour* 76, 131 – 134.

**Dykstra M.L. and Reuss L.E.** (2003) Electron Microscopy – Theory, techniques, and troubleshooting. *Springer* 2<sup>nd</sup> Edition, 288pp.

**Fironi P.** (1990) Our recent knowledge of the development of the cuttlefish (*Sepia officinalis*). *Zoologischer Anzeiger* 224, 1 – 25.

**Glauert A.M.** (1977) Staining methods for sectioned materials. North Holland. 547pp.

**Groeger G., Cotton P.A. and Williamson R.** (2005) Ontogenetic changes in the visual acuity of *Sepia officinalis* measured using the optometer response. *Canadian Journal of Zoology* 83, 274 – 279.

**Groeger G., Chrachri A. And Williamson R.** (2006) Changes in cuttlefish retinal sensitivity during growth. *Life and Environment* 56, 167 – 173.

**Hanlon R.G. and Messenger J.B.** (1998) Cephalopod Behaviour. Cambridge University Press. 248pp.

**Hara T. and Hara R.** (1965) New photosensitive pigment found in the retina of the squid *Ommastrephes*. *Nature* 206, 1331 – 1334.

**Hara T. and Hara R.** (1972) Cephalopod retinochrome. In Dartnall H.J.A. (eds) *Handbook of sensor physiology: photochemistry of vision*. Berlin: Springer-Verlag, pp. 720 – 746.

**Hara T. and Hara R.** (1976) Distribution of rhodopsin and retinochrome in the squid retina. *The Journal of General Physiology* 67, 791 – 805.

**Hara T., Hara R. and Takeuchi J.** (1967) Rhodopsin and retinochrome in the octopus retina. *Nature* 214, 572 – 573.

**Hariyama T., Meyer-Rochow V.B. and Eguchi E.** (1986) Diurnal changes in structure and function of the compound eye of *Ligia exotica* (Crustacea, Isopoda). *Journal of Experimental Biology* 123, 1 – 26.

**Kalil R.** (1978) Dark rearing in the cat: effects on visuomotor behaviour and cell growth in the dorsal lateral geniculate nucleus. *Journal of Comparative Neurology* 3, 451 – 467.

**Khosravi-Far R., Zakeri Z., Lockshin R.A. and Piacentini M.** (2008) Methods in enzymology – Programmed cell death, general principles for studying cell death Part A. *Academic Press* 442, pp. 550.

**Koueta E. and Boucaud-Camou E.** (2003) Combined effects of photoperiod and feeding frequency on survival and growth of juvenile cuttlefish *Sepia officinalis* L. in experimental rearing. *Journal of Experimental Marine Biology and Ecology* 296, 215 – 226.

**Land M.F.** (1981) Optics and vision in invertebrates. In Autrum H. (eds) *Handbook of sensory physiology*. Berlin: Springer-Verlag, pp. 471 – 592.

**Meinertzhagen I.A.** (1990) Development of the squids visual system. In Gilbert D.J., Adelman W.J. and Arnold J.M. (eds) *Squid as experimental animals*. Plenum Press.

**Muntz W.R.A. and Wentworth S.L.** (1987) An anatomical study of the retina of *Nautilus pompilius*. *Biological Bulletin* 173, 387 – 397.

**Naylor P.** (2005) Molluscs. In *Great British Marine Animals* (eds). Cornwall: Sound Diving Publications, pp. 152 – 157.

**Pepe I.M.** (2001) Recent advances in our understanding of rhodopsin and phototransduction. *Progress in Retinal and Eye Research* 20, 733 – 759.

**Siszik S. and Bilotta J.** (2001) Constant dark rearing effects on visual adaptation of zebrafish ERG. *International Journal of Developmental Neuroscience* 19, 611 – 619.

**Turner J.R., White E.M., Collins M.A., Partridge J.C. and Douglas R.H.** (2009) Vision in lanternfish (Myctophidae): adaptations for viewing bioluminescence in the deep sea. *Deep Sea Research I* Article in Press. pp.15

**Wells M.J.** (1958) Factors affecting reaction to *Mysis* by newly hatched *Sepia*. *Behaviour* 13, 96 – 111.

**West J.A., Sivak J.G. and Doughty M.J.** (1995) Microscopical evaluation of the crystalline lens of the squid (*Loligo opalescens*) during embryonic development. *Experimental Eye Research* 60, 19 – 35.

**Yamamoto M.** (1985) Ontogeny of the visual system in the cuttlefish, *Sepiella japonica*. I. Morphological differentiation of the visual cell. *The Journal of Comparative Neurology* 232, 347 – 361.

**Yamamoto T., Tasaki K., Sugawara Y. And Tonosaki A.** (1965) Fine structure of the octopus retina. *The Journal of Cell Biology* 25, 345 – 359.

**Young J.Z.** (1962) Light and dark adaptation in the eyes of some cephalopods. *Proceeding of the Zoological Society of London* 14, 255 – 273.